

AperTO - Archivio Istituzionale Open Access dell'Università di Torino

Biocompatible glass-ceramic materials for bone substitution

This is the author's manuscript

Original Citation:

Availability:

This version is available <http://hdl.handle.net/2318/101588> since

Terms of use:

Open Access

Anyone can freely access the full text of works made available as "Open Access". Works made available under a Creative Commons license can be used according to the terms and conditions of said license. Use of all other works requires consent of the right holder (author or publisher) if not exempted from copyright protection by the applicable law.

(Article begins on next page)

Biocompatible glass–ceramic materials for bone substitution

Chiara Vitale-Brovarone · Enrica Verné ·
Lorenza Robiglio · Germana Martinasso ·
Rosa A. Canuto · Giuliana Muzio

Received: 16 August 2006 / Accepted: 11 December 2006 / Published online: 3 July 2007
© Springer Science+Business Media, LLC 2007

Abstract A new bioactive glass composition (CEL2) in the $\text{SiO}_2\text{--P}_2\text{O}_5\text{--CaO--MgO--K}_2\text{O--Na}_2\text{O}$ system was tailored to control pH variations due to ion leaching phenomena when the glass is in contact with physiological fluids. CEL2 was prepared by a traditional melting-quenching process obtaining slices that were heat-treated to obtain a glass-ceramic material (CEL2GC) that was characterized thorough SEM analysis. Pre-treatment of CEL2GC with SBF was found to enhance its biocompatibility, as assessed by in vitro tests. CEL2 powder was then used to synthesize macroporous glass–ceramic scaffolds. To this end, CEL2 powders were mixed with polyethylene particles within the 300–600 μm size-range and then pressed to obtain crack-free compacted powders (green). This was heat-treated to remove the organic phase and to sinter the inorganic phase, leaving a porous structure. The biomaterial thus obtained was characterized by X-ray diffraction, SEM equipped with EDS, density measurement, image analysis, mechanical testing and in vitro evaluation, and found to be a glass–ceramic macroporous scaffold with uniformly distributed and highly interconnected porosity. The extent and size-range of the porosity can be tailored by varying the amount and size of the polyethylene particles.

Introduction

Since the discovery of bioglass by Hench et al. [1] in the early 1970s, various types of ceramic, glass and glass–ceramic have been proposed and used as bone replacement biomaterials [2–4]. Specifically, these biomaterials have found clinical applications as coating for prostheses, bone filler, vertebral substitution and, in a porous form, as bone substitutes [5–12]. Most of them are based on the $\text{SiO}_2\text{--P}_2\text{O}_5\text{--CaO--Na}_2\text{O}$ system. Bonding between bioactive glass or glass–ceramic and the surrounding tissues takes place through the formation of a hydroxyapatite layer, which is very similar to the mineral phase of bone. When the bioactive glass is placed in contact with physiological fluids, this layer is formed through a complex ion-exchange mechanism with the surrounding fluids, known as bioactivity. This biologically-active layer of hydroxyapatite can form on the surface of glasses having a wide compositional range, and is considered as self by the surrounding living tissue; its presence is widely recognized to be a sufficient requirement for the implant to chemically bond with the living bone. Kokubo et al. [13] proposed the Tris-buffered simulated body fluid (SBF) for the in vitro study of bioactive glass and glass–ceramic, since its ion concentration is almost equal to that of human blood plasma. Since then, in vitro tests in SBF have been widely used as preliminary tests on new candidate materials showing bioactive properties.

The ion leaching phenomenon involves the exchange of monovalent cations from the glass, such as Na^+ or K^+ , with H_3O^+ from the solution, and thus causes an increase in the pH of the solution. It is known that osteoblasts prefer a slightly alkaline medium (7.8) [14, 15], but it is also known that severe changes in pH can inhibit osteoblast activity and cause cell necrosis or apoptosis [16–18].

C. Vitale-Brovarone (✉) · E. Verné · L. Robiglio
Materials Science and Chemical Engineering Department,
Politecnico di Torino, Torino 10128, Italy
e-mail: chiara.vitale@polito.it

G. Martinasso · R. A. Canuto · G. Muzio
Department of Experimental Medicine and Oncology, University
of Turin, Torino, Italy

A new glass composition, named CEL2, was thus tailored, with the goal of avoiding large pH changes by giving the glass a lower monovalent oxide content (less than 20 mol%) and a slightly higher P_2O_5 content (3 mol%) compared to commercial bioactive glasses. Preliminary in vitro testing with osteoblast-like cells was carried out on the proposed glass, and it was also pre-treated in SBF for 1 week as a further control of pH variations, as has been proposed [18]. CEL2 was also used to prepare macroporous scaffolds for possible use as bone substitutes, through the burning-out method, described elsewhere [19]. This method involves the use of an organic phase as pore former, which is mixed with inorganic particles (CEL2 in this case) and then pressed, to obtain green, which is heat-treated to remove the organic phase and to sinter the inorganic phase.

Materials and methods

CEL2GC slice preparation

A new bioactive glass belonging to the system SiO_2 – P_2O_5 – CaO – MgO – Na_2O – K_2O was prepared. Its molar composition was selected so as to maximize bioactivity and biocompatibility, while avoiding undesired effects due to pH changes caused by the ion leaching phenomenon.

The synthesized glass, named CEL2, has the following molar composition: 45% SiO_2 , 3% P_2O_5 , 26% CaO , 7% MgO , 15% Na_2O , 4% K_2O , with a 4:1 Na_2O/K_2O ratio. The glass was prepared by melting reagent-grade reactants in a platinum crucible at 1400 °C for 1 h; the melt was poured onto a copper sheet to obtain bars, which were annealed at 500 °C for 12 h to release internal stresses. The bars were then cut into slices.

The molten glass was also poured into water to obtain a frit that was subsequently ball-milled to obtain powder. CEL2 powder was characterized through differential thermal analysis (DTA7 Perkins Elmer) to assess its characteristic temperatures.

CEL2 slices were heat-treated at 950 °C for 3 h to obtain glass–ceramic samples (CEL2GC) for purposes of comparison with the scaffolds, described below. CEL2GC slices were chemically etched using a 5 vol% 1:1 HF, HNO_3 solution to remove the amorphous phase and to investigate the morphology and composition of the crystalline phases.

Complete characterization of CEL2GC crystalline phases was attained through XRD analyses (X'Pert Philips Diffractometer), scanning electron microscopy (SEM Philips 525 M) and Energy Dispersive Spectroscopy (EDS). The glass–ceramic bioactivity was studied by soaking CEL2GC slices in 25 mL of SBF, a solution that simulates

the inorganic composition of human plasma [13]. In particular, CEL2GC slices were maintained at 37 °C for 1 week to study the formation of a silica rich gel layer and the precipitation of hydroxyapatite (HAp) microcrystals on top of that layer. During the test, the solution was refreshed every 48 h to simulate physiological fluid exchange. The pH of the solution was measured daily to evaluate the influence of ion exchange between the sample and SBF and to verify its confinement within a “physiological range”.

Scaffold preparation and characterization

CEL2 powders were used to synthesize scaffolds for bone substitutions. For this purpose, CEL2 powder was mixed with a thermally-degradable phase (polyethylene) of appropriate size, the mixture was then pressed and heat-treated to remove the organic phase and sinter CEL2 powders. Specifically, CEL2 powders were sieved through 106 μm mesh, and polyethylene (PE) particles in the 300–600 μm size-range were used as pore formers.

CEL2 powders and PE particles were mixed in a 1:1 volume ratio and pressed at 160 MPa for 10 s to obtain crack-free green bars of size $5 \times 1.5 \times 1.5$ cm. The bars were heat-treated at 950 °C for 3 h, heating rate 5°/min, obtaining a macroporous glass–ceramic structure. The bars were then cut into $1 \times 1 \times 1$ cm sample cubes, which were used to assess the compressive strength of the scaffolds; the test was performed in triplicate. The scaffold microstructure was observed under the SEM to investigate porosity and degree of sintering. The total porosity was studied in triplicate on sample cubes using the following formula:

$$\% P = (1 - W_m/W_{th}) \times 100 \quad (1)$$

where W_m is the measured weight and W_{th} the theoretical weight obtained by multiplying the density of the glass by the volume of the sample. The scaffold porosity was also investigated in triplicate through image analysis on cross-sections, with a window size of about $3 \text{ mm} \times 2 \text{ mm}$.

Scaffold bioactivity was studied by soaking sample cubes in SBF for 1 week, refreshing the solution every 48 h.

Biological tests

CEL2GC slices and CEL2GC slices pre-treated in SBF for 1 week were investigated to assess the influence of this pre-treatment on the biological response. A human osteoblast cell line (MG-63) obtained from the American Type Culture Collection (Rockville, MD, USA) was grown as a confluent monolayer in MEM medium containing 2 mM L-glutamine, 1% (v/v) antibiotic/antimycotic solution, 1 mM sodium pyruvate, and 10% (v/v) FBS (fetal bovine serum)

Fig. 1 Characterization of CEL2GC slices (a) rectangular shaped phase; (b) EDS of a; (c) needle shaped crystalline phase; (d) EDS of the needle shape crystalline phase of c

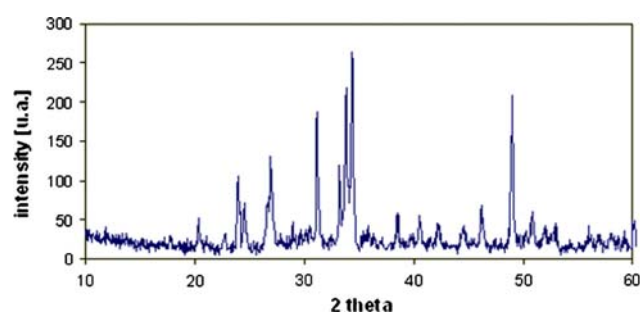
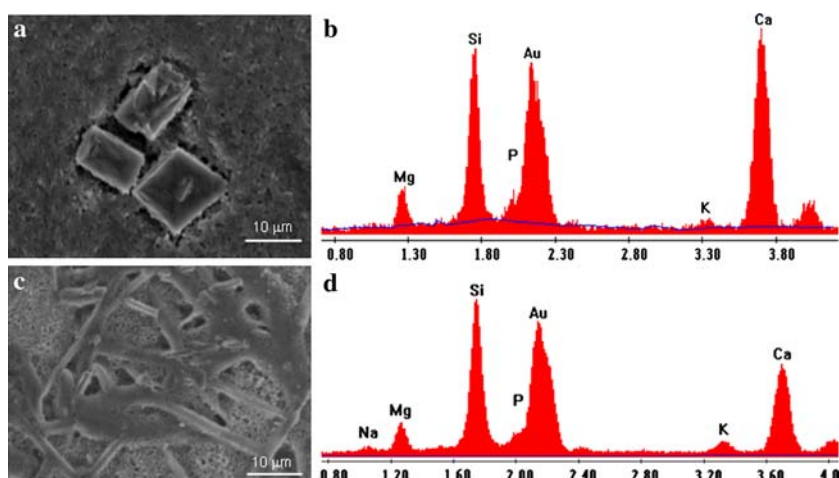


Fig. 2 Diffraction pattern of CEL2GC

under an atmosphere of 5% CO₂ and 95% air at 37 °C. The sterilized CEL2GC slices, pre-treated or not in SBF, were preconditioned for 24 h with culture medium in multi-well plates and used to grow MG-63 cells. After removing the preconditioning medium, the cells were seeded (10,000 cells/cm²) in multi-well plates containing the slices. Three and eight days after seeding the osteoblasts, the medium as well as the slices were removed. The slices were used to count the number of cells growing on them, and to examine the morphology of cells on the slices.

Cell growth and viability

To count the cells present on them, slices were treated with trypsin to detach cells; detached cells were harvested and centrifuged at 600 × g for 10 min. The cells were counted in a Burkert chamber using a light microscope (Leitz, Wetzlar, HM-LUX, Germany). To determine cell viability, plasma-membrane integrity was checked microscopically using the trypan blue exclusion test. Trypan blue exclusion was evaluated on cells suspended in the presence of the dye (0.8 mg/mL); 400 cells were counted for each sample and the result expressed as percentage of trypan blue-positive cells.

Morphological evaluation by SEM

After cell culture, the slices were rinsed four times in PBS and fixed with 2.5% glutaraldehyde in 0.1 M phosphate buffer, pH 7.4, for 30 min at 4 °C. Dehydration was performed with slow water replacement by a series of graded ethanol solutions with final dehydration in absolute ethanol before critical-point drying. A gold coating was then sputtered onto the samples for SEM observations.

Results and discussion

The TGA trace of CEL2 showed the presence of two exothermic peaks, implying the nucleation and growth of two different crystalline phases during the sintering treatment.

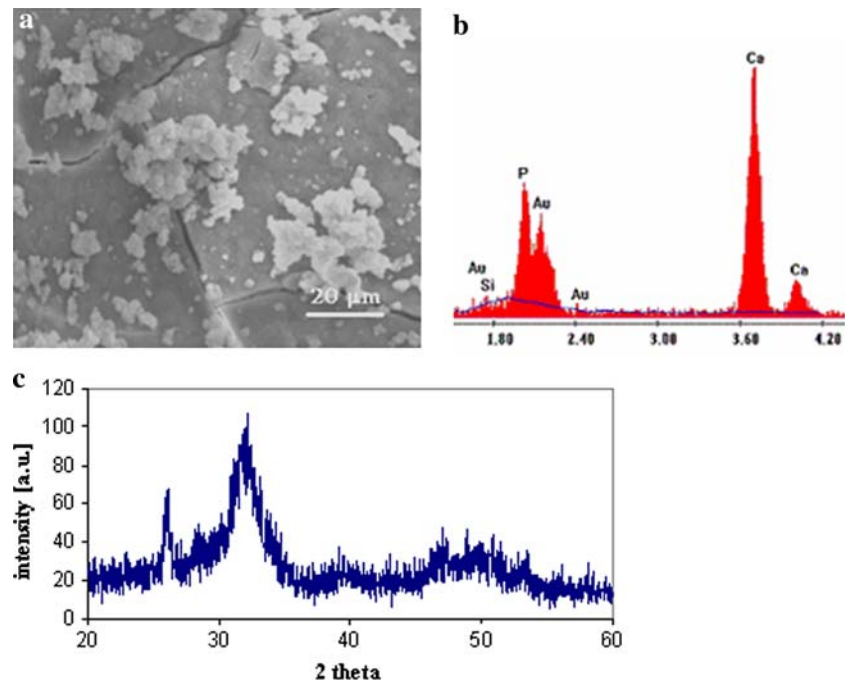
The use of CEL2 for the synthesis of macroporous structures involves heat-treatment above the crystallization temperature of CEL2 (T_{xx}) and thus a glass–ceramic structure was expected. In order to observe and evaluate the crystalline phase morphology and composition, CEL2 slices were heat-treated at 950 °C for 3 h obtaining glass–ceramic slices (CEL2GC).

CEL2GC slices were chemically etched with HNO₃/HF 5 vol% for 30 s to remove the residual amorphous phase to better observe the crystalline phases.

Figure 1a depicts the morphology of the first crystalline phase, which is tetragonal with sharp edges; the surrounding phase is the etched amorphous matrix with its typical indented aspect. Fig. 1b reports the EDS results for the tetragonal phase which, as may be seen, consists of a great amount of silicon, calcium and smaller quantities of magnesium.

The second crystalline phase is shown in Fig. 1c, it is needle shaped and the EDS results in Fig. 1d show that mainly comprises silicon, calcium, and magnesium. The

Fig. 3 Characterization of CEL2GC slices after pre-treatment in SBF (a) CEL2GC after 1 week of soaking in SBF; (b) EDS of the whole area of micrograph a; (c) Diffraction pattern of CEL2GC after 1 week in SBF



comparison between the two EDS results shows that the tetragonal phase is richer in calcium and poorer in silicon than the needle shaped phase. X-ray diffraction (X'Pert Philips Diffractometer) was used to assess the glass–ceramic nature of CEL2GC and to identify the crystalline structure of the two phases. The diffraction pattern obtained is reported in Fig. 2: the amorphous halo has almost disappeared and many diffraction peaks are present, as usually occurs for glass–ceramic materials. Due to the complex composition of the crystalline phases, correct identification of the peaks was impossible and thus, on the basis of the EDS analysis, we may only say that the two phases are calcium–magnesium silicates of different compositions.

CEL2GC bioactivity was investigated by soaking 1×1 cm glass–ceramic slices in 25 mL of SBF, refreshing

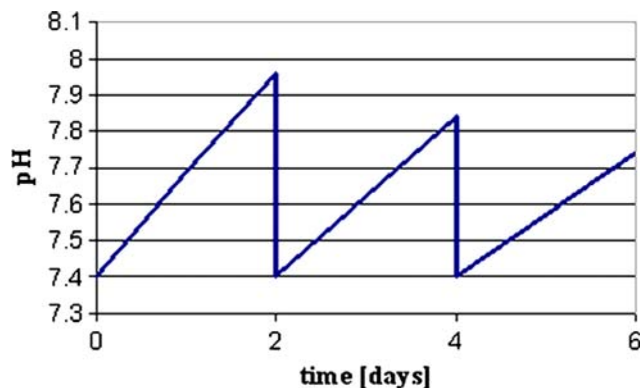


Fig. 4 pH variations induced by CEL2GC in SBF, refreshing the solution every 2 days

the solution every 2 days; refreshing the solution is frequently applied to more accurately simulate in vitro fluid circulation in the body.

Figure 3a reports a micrograph of CEL2GC after 1 week of soaking in SBF: the surface is completely covered by globular agglomerates of microcrystalline HAp. The EDS analysis confirmed that the entire surface was completely covered with HAp, since only phosphorus and calcium were detected, with a Ca/P ratio of 1.7. The layer beneath the HAp crystals is a gel-like layer rich in silica: the cracks that are visible are due to drying of this silica gel layer, which is highly hydrated; such cracks are frequently observed on bioactive surfaces after soaking in SBF.

X-ray diffraction analyses were carried out on CEL2GC slices after soaking in SBF to support the SEM and EDS observations. Figure 3c reports the obtained CEL2GC diffraction pattern after 1 week of soaking in SBF: as can be observed, only two very wide peaks were detected and their diffraction angles correspond to crystalline HAp. The absence of CEL2GC diffraction peaks after soaking in SBF is evidence of the thickness and uniformity of the HAp layer precipitated on the CEL2GC surface. The width of the diffraction peaks detected confirmed the microcrystalline nature of the HAp crystals, which is typical of those grown in vitro on the surface of bioactive materials. On these bases, CEL2GC may be considered a highly bioactive glass–ceramic.

The rate and amount of ion release, and the related pH variation, when a glass–ceramic is placed in contact with physiological fluids, are extremely important for its bio-

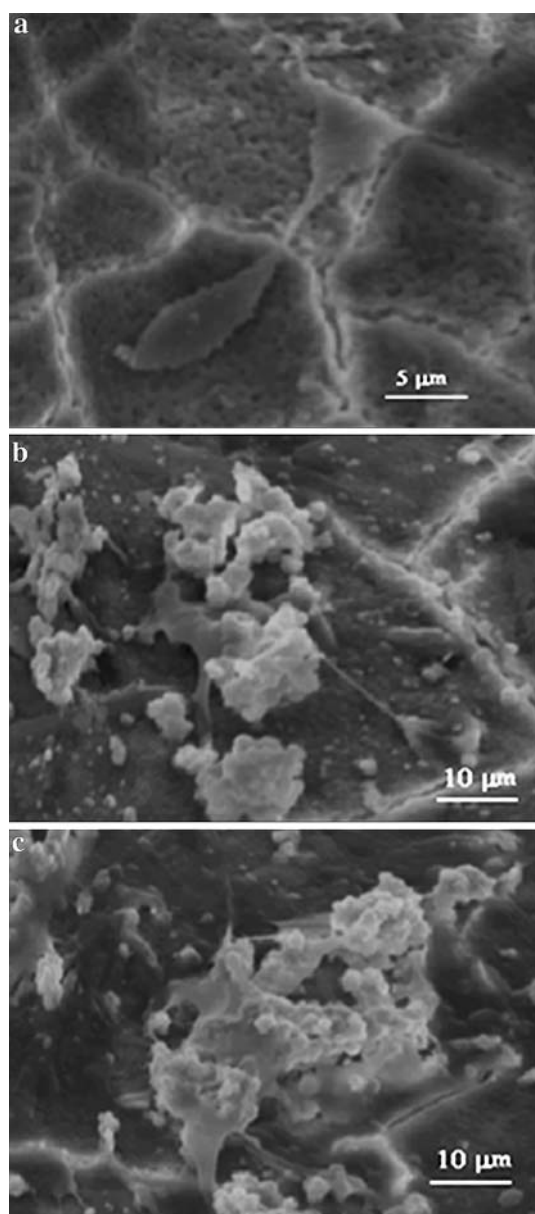


Fig. 5 Osteoblast morphology as assessed by SEM. Osteoblast proliferation for 8 days on as done CEL2GC (a); osteoblast proliferation for 8 days on CEL2GC after 1 week of pre-treatment in SBF (b, c)

compatibility. It is known that osteoblasts prefer moderately alkaline conditions, i.e. pH values close to 7.8, while changes in pH cause severe damage to cell viability [16–18]. CEL2 composition was tailored in light of this consideration, in an attempt to control pH variations. The total content of monovalent ions was thus kept below 20 mol% and the P_2O_5 content was set at 3 mol%, which is higher than most bioactive glasses reported in the literature.

pH variations were studied by soaking CEL2GC slices in SBF for 1 week, refreshing the solution every 2 days. Figure 4 reports the pH trend for CEL2GC during its

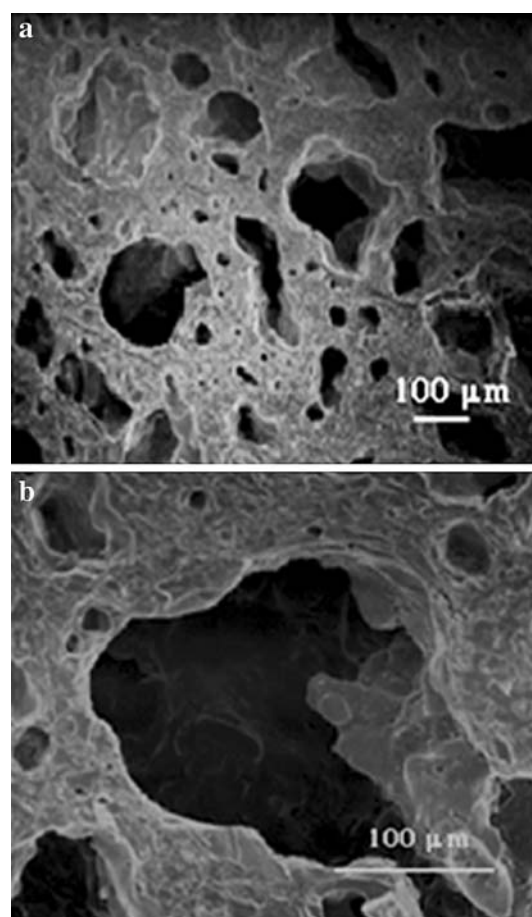


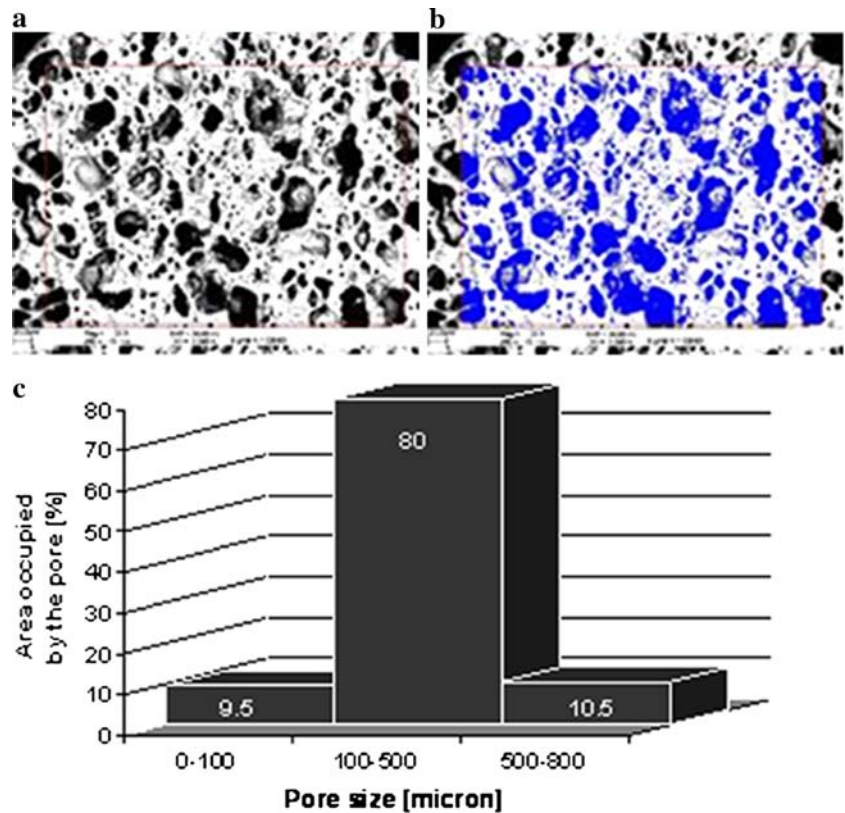
Fig. 6 Micrographs at SEM of a CEL2 scaffold cross-section (a); magnification of a CEL2 scaffold pore (b)

soaking in SBF. As can be observed, after 6 days of soaking in SBF, the pH is stable at around 7.75, which may be considered optimal for osteoblast adhesion and proliferation. The biocompatibility of CEL2GC was studied through biological tests using human osteoblast-like MG-63. For this purpose, CEL2GC slices and CEL2GC slices pre-treated in SBF for 1 week were tested, to determine any differences between them and any benefits relating to CEL2GC pre-treatment in SBF.

The cells grew better in CEL2GC slices pre-treated in SBF than they did in untreated CEL2GC slices, cell numbers increasing 3.5 fold between day 3 and day 8 of culture in pre-treated slices, versus 2.6 fold in untreated slices. Cell viability was the same in cells grown on both types of slice (data not shown).

Differences between the two types of slices were also investigated by SEM, determining cell morphology (Fig. 5). Figure 5a shows a human osteoblast-like MG-63 cell on CEL2GC after 8 days of culture, and Fig. 5b, c the same on slices pre-treated in SBF for 1 week. The better adhesion and spread of osteoblasts on CEL2GC pre-treated

Fig. 7 Pore evaluation of scaffolding. Selection of window size (a), detection of the open pores in the window (b); histogram of pore size distribution (c)



in SBF versus untreated slices is clear. Thus the response to CEL2GC pre-treated in SBF for 1 week was biologically more active than to CEL2GC as such. As may be seen, CEL2GC released ions into the culture medium, since its surface is irregular and etched. In the case of pre-treated CEL2GC, during pre-treatment in SBF considerable ion release occurred, leading to pH variations, chiefly in the first 2 or 3 days of soaking in SBF, with pH values reaching 8 (see Fig. 4). After 1 week of soaking, the solution being refreshed every 2 days, the pH variation reached a plateau at about 7.75, a level compatible with good cellular activity. In this case, the surface is covered by HAp crystals, as may be seen in Fig. 3, and cells anchor themselves onto these agglomerates, making bridges between the HAp microcrystals (see Fig. 5).

CEL2 was used to prepare macroporous glass–ceramic scaffolds. For this purpose, CEL2 powder sieved through 106 μm mesh was pressed with polyethylene particles in a size range of 300–600 μm , to obtain crack-free green, which was heat-treated to remove the organic phase and sinter the glass particles. Porous scaffolds were successfully obtained using 50% of polyethylene and 50% of CEL2 powder by volume. Figure 6a shows a cross-section of the scaffold obtained, in which the presence of a small number of macropores and diffuse microporosity may be seen. Microporosity is a key factor for nutrient flow inside the scaffold, and is also known to play a positive role on

proteins and cellular adhesion [20]. Figure 6b shows the scaffold at higher magnification; the high degree of sintering of the pore struts and the pore interconnection can be observed. The scaffold porosity was investigated through weight measurements using Eq. 1 obtaining a total porosity of $48 \pm 3 \text{ vol}\%$. The low standard deviation is a proof of the reproducibility of the proposed method.

Image analysis studies were carried out on the scaffold using a representative window size of a few mm^2 . An example of the results obtained is shown in Fig. 7. Specifically, Fig. 7a reports a back-scattering micrograph of a CEL2 scaffold cross-section and Fig. 7b reports the chosen window for pore evaluation. As may be seen in Fig. 7a, the pores are uniformly distributed along the cross-section and there is uniform dispersed microporosity. Image analysis showed an average pore size of 105 μm , across both micropores and macropores. Figure 7c is a histogram of the pore size distribution, considering not the number of pores but rather the area they occupy, which is directly related to the scaffold capability to host blood vessel formation, cell viability and nutrient flow in vivo. As may be seen, macropores in the range 100–500 μm account for most of the pore area, similarly manner to what occurs in human trabecular bone. It is agreed [21–25] that 100 μm is the lower size limit at which macropores enable a scaffold to provide cell migration and vascularisation; thus it may be said that the proposed scaffolds meet this requirement.

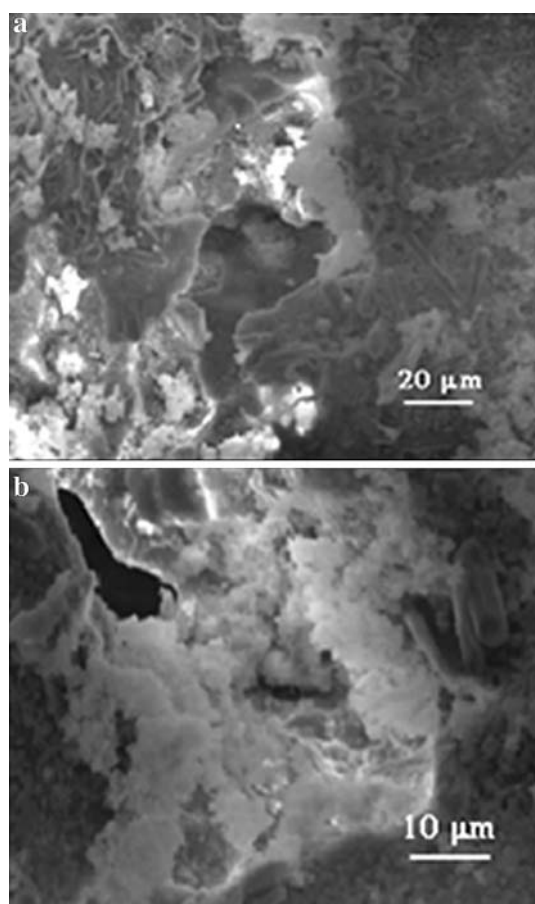


Fig. 8 SEM micrographs of the scaffold after 1 week in SBF

A compressive strength of 7 ± 0.6 MPa was determined for the sample cubes. This value is very similar to that of human cancellous bone, which varies within 2–12 MPa. A very low standard deviation was found, demonstrating the good reproducibility of the scaffold synthesis process.

Figure 8 shows two micrographs of the scaffold surface after 1 week of soaking in SBF. As can be observed in Fig. 8a, the scaffold surface is covered by many globular agglomerates that, as is visible at higher magnification (Fig. 8b) are also present on the pore walls. EDS analyses on the white agglomerates (data not reported) only showed the presence of Ca and P.

Conclusions

CEL2 in its glass–ceramic form was found to be a bioactive and highly compatible biomaterial. Pre-treatment in SBF for 1 week was found to be effective for favoring cell adhesion and proliferation. The good biological behavior of CEL2GC pre-treated in SBF, compared to untreated

CEL2GC, was shown by the increased osteoblast proliferation on pretreated slices, with formation of calcium deposits. The number and size of the calcium deposits increased with culture time, to a greater extent in pre-treated slices than in untreated ones, demonstrating the higher osteoblast activity in the presence of a surface covered with HAp crystals.

CEL2 powders were successfully used to prepare scaffolds using the polymeric burning-out method: the pores present a certain degree of interconnection and most are in the 100–500 µm range, which is considered optimal for a bone replacement.

The compressive strength of the scaffold (7 MPa) is in the range of human trabecular bone and the low standard deviation confirmed the reproducibility of the proposed method.

Work is in progress on the use of CEL2 to prepare scaffolds with the polymeric replication method in order to obtain a pore structure closer to that of human bone, both in terms of interconnection and pore-size distribution.

Acknowledgment This work was supported by grants from Regione Piemonte and University of Turin, Italy.

References

1. L. L. HENCH, R. J. SPLINTER, W. C. ALLEN and T. K. GREENLEE, *J. Biomed. Mater. Res.* **2** (1971) 117
2. H. OONISHI, L. L. HENCH, J. WILSON, F. SUGIHARA, E. TSUJI, M. MATSUURA, S. KIN, T. YAMAMURO and S. MI-ZOKAWA, *J. Biomed. Mater. Res.* **51** (2000) 37
3. P. DUCHEYNE and J. M. CUCKLER, *Rev. Clin. Ortho. Rel. Res.* **277** (1992) 102
4. M. VALLET-REGI, *J. Chem. Soc. Dalton Trans.* **5** (2001) 97
5. E. VERNÈ, M. BOSETTI, C. VITALE-BROVARONE, C. MOISESCU, F. LUPO, S. SPRIANO and M. CANNAS, *Biomaterials* **23** (2002) 3395
6. E. VERNÈ, R. DEFILIPPI, G. CARL, C. VITALE-BROVARONE and P. APPENDINO, *J. Eur. Cer. Soc.* **23** (2003) 675
7. C. Vitale-Brovarone, S. Di Nunzio, O. Bretcanu, E. Vernè, *J. Mat. Sci. Mat. Med.* **15** (2004) 209
8. E. VERNÈ, F. VALLES, C. VITALE-BROVARONE, S. SPRIANO and C. MOISESCU, *J. Eur. Cer. Soc.* **24** (2004) 2699
9. C. VITALE-BROVARONE and E. VERNÈ, *J. Mat. Sci. Mat. Med.* **16** (2005) 863
10. J. E. GOUGH, J. R. JONES and L. L. HENCH, *Biomaterials* **25** (2004) 2039
11. I. JUN, Y. KOH and H. KIM, *J. Am. Cer. Soc.* **89** (2006) 391
12. M. M. PEREIRA, J. R. JONES and L. L. HENCH, *Adv. App. Cer.* **104** (2004) 35
13. T. KOKUBO, H. KUSHITANI and S. SAKKA, *J. Biomed. Mater. Res.* **24** (1990) 721
14. W. K. RAMP, L. G. LENZ and K. K. KAYSINGER, *Bone Miner.* **24** (1994) 59
15. K. K. KAYSINGER and W. K. RAMP, *J. Cell Biochem.* **68** (1998) 83
16. A. BRANDAO-BURCH, J. C. UTTING, I. R. ORRISS and T. R. ARNETT, *Calcif. Tissue Int.* **77** (2005) 167

17. K. K. FRICK, L. JIANG and D. A. BUSHINSKY, *Am. J. Physiol.* **272** (1997) C1450
18. A. EL-GHANNAM, P. DUCHEYNE and I. SHAPIRO, *Biomaterials* **18** (1997) 295
19. C. VITALE-BROVARONE, E. VERNÈ, P. APPENDINO, *J. Mat. Sci. Mat. Med.* **17** (2006) 1069
20. J. GOUGH, J. JONES and L. L. HENCH, *Biomaterials* **25** (2004) 2039
21. H. R. RAMAY and M. ZHANG, *Biomaterials* **24** (2003) 3293
22. O. GAUTHIER, J. M. BOULER, E. AGUADO, P. PILET and G. DACULSI, *Biomaterials* **19** (1998) 133
23. J. R. JONES and L. L. HENCH, *Curr. Op. Sol. State Mat. Sci.* **7** (2003) 301
24. J. DONG, T. UEMURA, Y. SHIRASAKI and T. TATEISHI, *Biomaterials* **23** (2002) 4493
25. V. KARAGEORGIOU and D. KAPLAN, *Biomaterials* **26** (2005) 5474